

Cavity-induced quantum droplets

Leon Mixa,^{1,2,*} Milan Radonjić,^{1,3} Axel Pelster,⁴ and Michael Thorwart^{1,2}

¹*Institut für Theoretische Physik, Universität Hamburg, Notkestraße 9, 22607 Hamburg, Germany*

²*The Hamburg Center for Ultrafast Imaging, Luruper Chaussee 149, 22761 Hamburg, Germany*

³*Institute of Physics Belgrade, University of Belgrade, Pregrevica 118, 11080 Belgrade, Serbia*

⁴*Physics Department and Research Center OPTIMAS,*

Rheinland-Pfälzische Technische Universität Kaiserslautern-Landau,

Erwin-Schrödinger Straße 46, 67663 Kaiserslautern, Germany

(Dated: October 1, 2024)

Quantum droplets are formed in quantum many-body systems when the competition of quantum corrections with the mean-field interaction yields a stable self-bound quantum liquid. We predict the emergence of a quantum droplet when a Bose-Einstein condensate is placed in an optical resonator with transverse pumping. The strong coupling between the atoms and the cavity mode induces long-range interactions in the atoms and a roton mode for negative cavity detuning emerges. Using a Bogoliubov theory, we show that the roton mode competes with the repulsive atomic s -wave scattering. Due to the favorable scaling of the quantum fluctuations with respect to the volume, a self-bound stable quantum liquid emerges.

Introduction. Superfluid Helium-4 is known for intricate macroscopic quantum states most famous of which are probably the superfluid states [1] alongside the roton mode in its dispersion relation [2]. It also realizes a remarkable state of zero pressure at a specific density as a free droplet state [3]. Since liquid helium is highly correlated, the specific long-range correlations and the quantum many-body interactions that give rise to these properties are not easy to reveal. Progress has been achieved by constructing effective energy functionals [4–7] and by benchmarking them to experimental data rather than using first principles. That a quantum liquid of volume V and particle number N is self-confining in free space can ultimately be reduced to three conditions that its effective energy $E_0(V, N)$ has to fulfill [3]. The first one (C1) corresponds to finding a local extremum defined by $(\partial E_0/\partial V)_N = 0$ that determines the equilibrium system size V_0 . This becomes the zero-pressure condition in the thermodynamic limit. For stability, (C2) the local extremum must be a minimum, i.e., $(\partial^2 E_0/\partial V^2)_N|_{V=V_0} > 0$, which translates to positive bulk compressibility in the thermodynamic limit. And, finally, (C3) the droplet should not self-evaporate, i.e., $(\partial E_0/\partial N)_{V_0} < 0$, which relates to a negative effective chemical potential in the thermodynamic limit. A generic minimal model that can fulfill these conditions is provided by the effective energy $E_0 = \alpha V^{-1} + \beta V^{-1-\gamma}$. It turns out that three choices of parameters α , β , and γ can obey the droplet conditions (C1) and (C2). They are (D1) $\alpha < 0$, $\beta > 0$, $\gamma > 0$, (D2) $\alpha > 0$, $\beta < 0$, $0 > \gamma > -1$, and (D3) $\alpha > 0$, $\beta > 0$, $\gamma < -1$. Whether also the third condition (C3) is fulfilled depends on the specific N -dependence of α and β .

Recently, quantum droplets have been established as a new quantum state of matter. Unlike Helium droplets, they are realized in weakly interacting dilute atom gases, making them much easier to study theoretically. Their

discovery in Bose-Bose mixtures was sparked by the seminal theoretical prediction of Petrov [8] that, in such a system, the competition between intra- and inter-species contact interactions can cause the mean-field energy functional to become unstable. At the same time, the zero-point motion of the Bogoliubov excitations of the mixture, captured by the Lee-Huang-Yang (LHY) corrections [9], stabilizes the system. For a given particle density n , the competition between the unstable mean-field energy $\propto n^2$ and the stabilizing LHY term $\propto n^{5/2}$ establishes an equilibrium for which the system pressure vanishes for finite n in the thermodynamic limit. Such a droplet realization is of the type (D1). These self-bound quantum droplets of finite size are described by an extended Gross-Pitaevskii equation, where the LHY corrections are incorporated via a local density approximation [8]. Experimental realizations of quantum droplets were not only reported in Bose-Bose mixtures [10–12] but likewise in dilute Bose gases with dipolar interaction [13–15]. The extended Gross-Pitaevskii equation including the dipolar LHY correction [16–18] also serves as the theoretical framework for their description [19, 20]. Importantly, dipolar BECs host the roton mode, which was predicted in 2003 [21, 22] and later verified experimentally [23, 24]. This mode is related to phase-coherently coupled quantum droplets realizing a supersolid state of matter [25–27], which exists only in a narrow parameter window for sufficiently large N . Apart from three-dimensional quantum droplets, also two- and one-dimensional ones are studied [28–30]. One-dimensional mixture droplets represent an effective model adhering to (D2) [28].

When a three-dimensional Bose-Einstein condensate (BEC) is placed in an optical cavity, the Dicke model of cavity QED is realized [31, 32]. A transverse pump beam off-resonantly drives internal transitions of the atoms [33]. The quantum states of the cavity and the atoms are strongly coupled by the scattering of the pump photons

into the cavity and the repeated scattering of the cavity photons by the atoms [34]. For strong enough coupling, the cavity mediates a long-range effective atom-atom interaction which triggers a self-organization and the Dicke quantum phase transition [31, 32, 35] together with a softening of a roton-like mode of the atom gas [36].

In this Letter, we show that the quantum fluctuations of the roton mode give rise to the formation of quantum droplets. The mechanism differs in several aspects from that observed in either a mixture or a dipolar Bose gas. In those scenarios, the contact atom-atom interactions are tuned via Feshbach resonances so that the system becomes unstable at the mean-field level and the atomic quantum fluctuations stabilize the macroscopic state, corresponding to either the (D1) or (D2) class of droplet formation. For cavity-induced quantum droplets, in contrast, we show that a mean-field stable BEC in a cavity can rather form a quantum droplet for experimentally realistic densities due to destabilizing quantum fluctuations of the cavity mode. The competing terms in the effective energy realize the formation of a quantum droplet of type (D3), i.e., $\alpha > 0$, $\beta > 0$, and $\gamma < -1$. By varying the cavity parameters, the properties of the cavity-induced quantum droplet become tunable.

Cavity BEC model. The experimental setup is shown in the inset of Fig. 1. A BEC of atoms (with mass M of a single atom) in the ground state $|g\rangle$ of density n , with the contact interaction strength $g = 4\pi a_s/M$ ($\hbar = 1$) being determined by the s -wave scattering length a_s , is exposed to a pump beam of frequency ω_P along the y -axis. It drives an internal transition $|g\rangle \leftrightarrow |e\rangle$ of frequency ω_A with a large detuning $\Delta_A = \omega_P - \omega_A$. The beam has a broad envelope profile with a spatially dependent Rabi frequency $h(\mathbf{r}) = h_0 \cos ky$ with k being the wavenumber of the pump photon. The atoms are coupled to a quantized cavity mode of frequency ω_C whose axis is in the x -direction. The cavity mode is red detuned from the pump with $\Delta_C = \omega_P - \omega_C < 0$ and damped at the rate κ . The maximal Rabi frequency \mathcal{G}_0 determines the maximal effective coupling strength $U_0 = \mathcal{G}_0^2/\Delta_A$ between an atom in the $|g\rangle$ state and the cavity. We consider the TEM₀₀ mode $\mathcal{G}(\mathbf{r}) = \mathcal{G}_0 \cos(kx) \exp[-(y^2 + z^2)/\xi^2]$ with the Gaussian envelope of waist ξ transverse to the cavity axis. This results in a spatially dependent atom-cavity interaction [37]. We assume the hierarchy of parameter $|\Delta_A| \gg |\Delta_C| \gg \omega_R = k^2/(2M) \gg gn, |U_0|$, consistent with contemporary experimental setups. Here, ω_R is the atomic recoil frequency. This allows to eliminate both the excited atomic state $|e\rangle$ and the fast cavity mode [34, 37]. After resolving the ambiguities in the operator ordering [38], an effective atom-only Hamiltonian [39]

$$\hat{H}_{\text{eff}} = \int_V d^3\mathbf{r} \hat{\psi}^\dagger(\mathbf{r}) \left[-\frac{\nabla^2}{2M} + \frac{g}{2} \hat{\psi}^\dagger(\mathbf{r})\hat{\psi}(\mathbf{r}) \right] \hat{\psi}(\mathbf{r}) + \frac{1}{2} \int_V d^3\mathbf{r} \int_V d^3\mathbf{r}' \hat{\psi}^\dagger(\mathbf{r})\hat{\psi}(\mathbf{r}) V_C(\mathbf{r}, \mathbf{r}') \hat{\psi}^\dagger(\mathbf{r}')\hat{\psi}(\mathbf{r}') \quad (1)$$

results, where $\hat{\psi}(\mathbf{r})$ is the atomic ground state field operator. The cavity-induced atom-atom interaction reads

$$V_C(\mathbf{r}, \mathbf{r}') = \mathcal{I} \cos(kx) \cos(ky) e^{-(y^2+z^2)/\xi^2} \times \cos(kx') \cos(ky') e^{-(y'^2+z'^2)/\xi^2}, \quad (2)$$

where cavity and pump parameters lead to the effective interaction strength $\mathcal{I} = 2\mathcal{G}_0^2 h_0^2 \Delta_C / [\Delta_A^2 (\Delta_C^2 + \kappa^2)] < 0$.

Homogeneous mean-field approach. We assume that the atoms are placed in the cavity inside a cube of volume $V = L^3$ with $L < \xi$. Below the superradiant Dicke phase transition, the cavity remains empty and the condensate is homogeneous at the mean-field level [40]. In the second line of Eq. (1), an integral of the type [39]

$$\int_{-L/2}^{L/2} du e^{ipu} e^{-u^2/\xi^2} \approx \delta_{p0} \sqrt{\pi} \xi \operatorname{erf}\left(\frac{L}{2\xi}\right), \quad (3)$$

would appear then. The above approximation is quite accurate for $L < \xi$. For $k \neq 0$ there is no contribution of the cavity-induced interaction to the homogeneous mean-field energy, so that we may assume a uniform condensate $\langle \hat{\psi}(\mathbf{r}) \rangle = \sqrt{n}$. Hence, the cavity occupancy is directly related to the BEC (in)homogeneity. Thus, the mean-field energy obtained from Eq. (1) is that of a uniform condensate

$$E_{\text{mf}} = V \frac{g}{2} n^2. \quad (4)$$

Below the Dicke transition, the homogeneous mean-field condensate and its stability are unaffected by the cavity.

Quantum fluctuations. Next we develop a Bogoliubov theory of the fluctuations $\hat{\phi}(\mathbf{r}) = \hat{\psi}(\mathbf{r}) - \sqrt{n}$ around the homogeneous mean-field using the plane wave expansion $\hat{\phi}(\mathbf{r}) = \sum_{\mathbf{p} \neq 0} \hat{\phi}_{\mathbf{p}} e^{i\mathbf{p}\mathbf{r}} / \sqrt{V}$ and Eq. (3) for the cavity-induced interaction. Importantly, the cavity couples only to the four Bogoliubov modes $\mathcal{K}_C = \{(\pm k \pm k \ 0)^T\}$ determined k and the cavity mode functions. The remaining atomic modes not coupled to the cavity have the standard Bogoliubov dispersion $\omega_{\mathbf{p}} = \sqrt{\mathbf{p}^2/(2M)[\mathbf{p}^2/(2M) + 2gn]}$ in accordance with the Goldstone theorem. Their zero-point fluctuations in the continuum limit yield the LHY energy correction $8VM^{3/2}(gn)^{5/2}/(15\pi^2)$ [9]. For a dilute weakly interacting atom gas with $a_s^3 n \ll 1$ the LHY energy is negligibly small compared to the mean-field energy Eq. (4) and can be discarded.

The four modes of \mathcal{K}_C form a set of mutually interacting quantum harmonic oscillators with eigenfrequencies $\{\omega_{\mathbf{k}}, \omega_{\mathbf{k}}, \omega_{\mathbf{k}}, \Omega\}$ [39], where

$$\Omega = \sqrt{\omega_{\mathbf{k}}^2 + 16 \frac{k^2}{M} V_C(\mathbf{k}, \mathbf{k}) n} \quad (5)$$

denotes the frequency of the roton mode. It involves via Eq. (3) the Fourier transform of the cavity-mediated

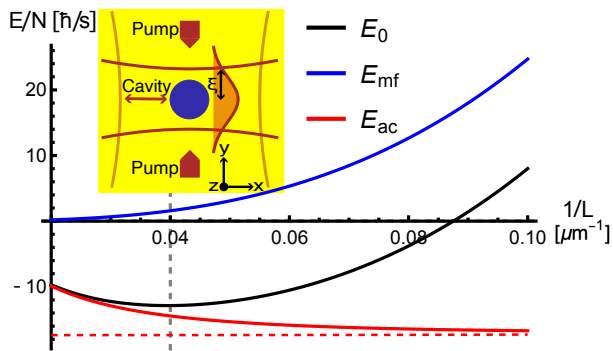


FIG. 1. Effective ground-state energy per atom E_0/N with its mean-field (E_{mf}) and cavity-induced (E_{ac}) quantum fluctuation contributions plotted against the inverse cloud size L for fixed atom number $N = 10^3$. The vertical gray dashed line marks the energy minimum corresponding to the equilibrium droplet size L_0 . The red dashed line indicates $E_{\text{ac}}^{(\infty)}$ for an infinite-range cavity $L/\xi \rightarrow 0$. Other parameters are $\mathcal{I} = 0.95 \mathcal{I}_{\text{cr}}$, $\xi = 50 \mu\text{m}$, $a_s = 100 a_0$, and $M = 87 u$. Inset: Three-dimensional BEC (in blue) placed at the cavity center aligned along the x -axis with a Gaussian mode profile of waist ξ . The broad pump laser propagates along the y -direction.

interaction potential

$$V_C(\mathbf{p}, \mathbf{p}') = \frac{\mathcal{I}V}{32} \left[\frac{\sqrt{\pi}\xi}{L} \text{erf}\left(\frac{L}{2\xi}\right) \right]^4 \sum_{\mathbf{k}, \mathbf{k}' \in \mathcal{K}_C} \delta_{\mathbf{p}\mathbf{k}} \delta_{\mathbf{p}'\mathbf{k}'}. \quad (6)$$

The roton softness is determined by the effective cavity-induced interaction strength \mathcal{I} . It can be tuned by changing the pump strength h_0 or the cavity detuning Δ_C , but can also be fine-tuned by adopting any other cavity feature. The roton mode is responsible for the leading-order energy contribution

$$E_{\text{ac}} = \frac{1}{2} (\Omega - \omega_{\mathbf{k}}) \quad (7)$$

of the cavity quantum fluctuations [39], which corresponds to the difference between the respective energies with and without coupling to the cavity and vanishes in the limit $\mathcal{I} \rightarrow 0$. Combining Eq. (4) with Eq. (7) yields the effective beyond-mean-field energy $E_0 = E_{\text{mf}} + E_{\text{ac}}$ of the condensate ground state. The chemical potential then follows as $\mu_0 = gn + (\partial E_{\text{ac}}/\partial N)_V$.

Results. The formation of quantum droplets can be understood from analyzing E_0 . For fixed N , (C1) and (C2) impose that the system exhibits an energy minimum with respect to the volume V [41]. For repulsive contact interaction, the BEC mean-field energy Eq. (4) is positive and convex with respect to V . Conversely, due to $\Delta_C < 0$, which implies $\mathcal{I} < 0$, the contribution of the cavity quantum fluctuations Eq. (7) turns out to be negative, which is typical for a roton mode. Thus, adding Eqs. (4) and (7) can lead to an energetic minimum as depicted in Fig. 1. To maintain the homogeneous phase, we need to stay below the Dicke phase transition. Since the latter occurs

when the roton mode becomes soft, we derive the critical value $\mathcal{I}_{\text{cr}} = -2[(k^2/M) + 2gn]/N(\sqrt{\pi} \text{erf}[L/2\xi]\xi/L)^4$ from the condition $\Omega = 0$. The emergence of E_{ac} from a single roton mode has an important physical implication. In the thermodynamic limit, $N, L, \xi \rightarrow \infty$, while $N/V = \text{const.}$ and $L/\xi = \text{const.}$ Furthermore, the coupling of a single atom to the cavity vanishes, i.e., $\mathcal{G}_0 \rightarrow 0$, so that $\mathcal{I}V = \text{const.}$ holds. This renders the roton's energy contribution intensive, i.e., a *finite-size effect*. Consequently, in the limit of large N , the largest possible magnitude of E_{ac} , at $\Omega = 0$, will eventually be dwarfed by any extensive energy term. Hence, self-bound droplets are only possible for systems of finite size.

To gain further understanding, we expand $V_C(\mathbf{p}, \mathbf{p}')$ in Eq. (6) around $L/\xi = 0$ to the second order. Restricting to $L/\xi < 1$, this expansion is accurate for an experimental setup. The cavity quantum fluctuation correction is then expanded as $E_{\text{ac}} \approx E_{\text{ac}}^{(\infty)} + DL^2/2$. The first term $E_{\text{ac}}^{(\infty)}$ is the infinite interaction range energy correction, for $L \ll \xi$, indicated by the dashed horizontal line in Fig. 1. It does not depend on L and is equivalent to taking the zeroth order approximation in $1/\xi$ of the Gaussian envelope of $\mathcal{G}(\mathbf{r})$. By this, we recover the known results for the infinite-range cavity-induced interaction. The second term, resulting from the specific shape of the envelope, contains the factor $D = -\mathcal{I}N/[12\xi^2\sqrt{1+(4gn+\mathcal{I}N)M/(2k^2)}]$. We discard all contact interaction $gn \ll k^2/M$ in E_{ac} which is only invalid around $\mathcal{I} \lesssim \mathcal{I}_{\text{cr}}$. Then this term has the form of a harmonic-like self-trapping potential as it is proportional to L^2 . Therefore, the effective energy reads

$$E_0(N, V) = E_{\text{ac}}^{(\infty)} + \frac{gN^2}{2V} - \frac{\mathcal{I}NV^{2/3}}{24\xi^2\sqrt{1+\mathcal{I}NM/(2k^2)}}, \quad (8)$$

and gives rise to the equilibrium droplet volume $V_0^{5/3} = -18gN\xi^2\sqrt{1+\mathcal{I}NM/2k^2}/\mathcal{I}$. This corresponds to the minimal droplet model of type (D3) by identifying $\alpha = gN^2/2 > 0$, $\beta = D/2 > 0$, and $\gamma = -5/3$.

As stated in (C1) and (C2), energy minimization with respect to the system size translates into a zero pressure condition $0 = -(\partial E_0/\partial V)_N = P_0$ with positive bulk compressibility $0 < K(P_0 = 0) = -V(\partial P_0/\partial V)_N|_{V=V_0}$, corresponding to a thermodynamically stable state [3]. The mean-field contact interaction yields a positive pressure $P_{\text{mf}} = gn^2/2$, while the roton mode corresponds to a negative pressure $P_{\text{ac}} = -D/(3L)$. As the cavity-induced interaction becomes stronger with increasing \mathcal{I} , the negative pressure P_{ac} becomes comparable to the positive mean-field pressure P_{mf} . Their interplay results in a stable droplet with zero total pressure and positive bulk compressibility, as displayed in Fig. 1. The compressibility also obeys $K(P_0 = 0)/n < gn$. The corresponding sound velocity $c_s = \sqrt{K(P_0 = 0)/(Mn)}$ is modified by the roton mode contribution and turns out to be reduced with respect to the homogeneous counterpart $\sqrt{gn/M}$.

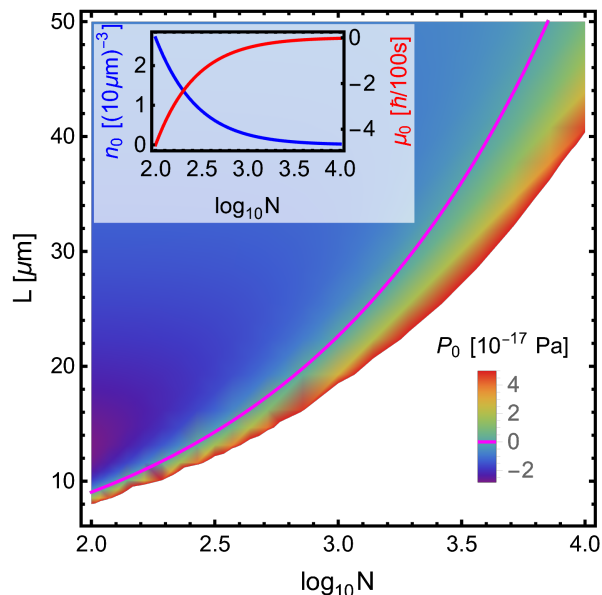


FIG. 2. System pressure P_0 dependence on the atom number N and the system size L for $\mathcal{I} = 0.95 \mathcal{I}_{\text{cr}}$. The magenta line marks zero pressure. Inset: Droplet density (blue) and chemical potential (red) realized along this line. The absolute value of \mathcal{I} decreases as N increases. Remaining parameters as in Fig. 1.

The resulting system pressure is depicted in Fig. 2 for varying particle number N and system size L . The magenta line marks $P_0 = 0$, where the droplet size $L_0 = V_0^{1/3}$ is determined by N and other system parameters. We find negative pressure above this line and positive pressure below it, indicating the positive bulk compressibility $K(P_0 = 0)$ for the droplet corresponding to each atom number N . The inset shows the equilibrium density n_0 realized along the zero pressure line. As the number of particles increases, the droplet density decreases monotonically. The decrease is mainly caused by keeping the cavity interaction $\mathcal{I} = 0.95 \mathcal{I}_{\text{cr}}$ fixed due to $\mathcal{I}_{\text{cr}} \propto N^{-1}$. In principle, denser droplets can be realized by getting closer to the Dicke phase transition [39]. This is due to the divergence of the cavity pressure P_{ac} when the roton mode vanishes as $\mathcal{I} \rightarrow \mathcal{I}_{\text{cr}}$. We note that the roton divergence goes along with the diverging condensate depletion into the roton mode. In line with contemporary experiments, we have chosen to stay 5% below the critical point. With this we extract the leading order relation $V_0 \sim N^{3/5}$ from our analytical expression for V_0 .

Finally, we check whether the chemical potential remains negative [3] such that the droplet does not evaporate spontaneously, i.e., we analyze $[E_0(N-1) - E_0(N)]/N|_{P_0=0} > 0$. The total chemical potential $\mu_0 = gn + (\partial E_{\text{ac}}/\partial N)_V$ is composed of the positive mean-field and the negative roton contribution, respectively. At zero pressure, the cavity-induced term prevails over gn , resulting in a negative overall $\mu_0(P_0 = 0) < 0$, thus avoiding

self-evaporation [39]. As displayed in Fig. 2 (inset), the absolute value of the total chemical potential diminishes for growing N in the same way as the density. Yet, it always remains negative.

Quantitative examination of the results in Figs. 1 and 2 reveals that, compared to typical BEC atom numbers and other droplet realizations [10–14], the droplet densities presented here are orders of magnitude more dilute. This roots in the BEC mean-field contact interaction that the cavity fluctuations have to overcome. In other droplet realizations, the mean field is almost completely suppressed from the outset. In addition, the homogeneous nature of the droplets is constrained by the Dicke phase transition. Droplets of any desired density can be obtained by approaching the Dicke critical point. However, due to technical limitations in experimental control, it is more viable to optimize other system parameters, such as, e.g., the equilibrium density which scales approximately as $n_0 \sim g^{-3/5}$ with respect to the contact interaction strength [39]. It is also possible to optimize the setup with respect to the cavity mode width and explore the dependence $n_0 \sim \xi^{-6/5}$ [39].

Although we have focused on the simplest form of a cavity-induced long-range interaction, the theory can account for any envelope function $f(\mathbf{r}, \mathbf{r}')$ and system dimension. However, analytical solvability requires the existence of an approximation of the envelope Fourier transform as in Eq. (3). Our theory, e.g., can easily be applied [39] to multimode cavities with an envelope $f(x, x') = \exp[-(x-x')^2/\xi^2]$ [34]. Those have been studied in a lattice with quantum Monte Carlo techniques [42] and in terms of numerical solutions for ring cavities [43].

Conclusions. We have shown that a mean-field stable uniform BEC can be turned into a stable quantum droplet when coupled to a single-mode cavity with transverse pumping. The zero-point energy of the cavity quantum fluctuations provides a stabilizing attractive quantum correction to the mean-field BEC contact interaction energy for negative cavity detuning. The dependence of the attractive term on the BEC volume is crucially influenced by the shape of the cavity mode function, which determines the cavity-induced atom-atom interaction potential Eq. (2). The Fourier transform of the mode function envelope determines the roton eigenfrequency and thus the finite-size behavior of the roton energy contribution. An alternative view is that the cavity quantum fluctuations, once strongly coupled to the BEC, exert a significant negative pressure on the atomic cloud.

The equilibrium density of cavity-induced quantum droplets can be tuned by varying external cavity parameters, such as the strength of the transverse pump or the cavity detuning. The self-boundness should be the key experimental fingerprint of these quantum objects. If a BEC is prepared, coupled to the cavity, and then released by removing the confinement, the self-bound nature could be revealed by absorption imaging whether the

cloud maintains its volume or expands. Finally, we note that the thermal pressure in the low-temperature limit $P_{\text{th}} = M^{3/2}\pi^2(k_{\text{B}}T)^4/[90(gn)^{3/2}]$ would contribute in an experimental implementation. However, any realization would be based on the principal mechanism that the cavity quantum fluctuations realize competing interactions in the atoms that is fundamentally different from other quantum droplets and falls into the category (D3) in our classification.

Acknowledgments. We are grateful to Andreas Hemmerich and Hans Kessler for helpful discussions on the experimental parameters. This work was supported by the Deutsche Forschungsgemeinschaft (DFG, German Research Foundation) via the Collaborative Research Center SFB/TR185 (Project No. 277625399) (A.P.) and via the Research Grant No. 274978739 (M.R. and M.T.). We also acknowledge the support from the DFG Cluster of Excellence CUI: “Advanced Imaging of Matter” – EXC 2056 (Project ID 390715994).

* leon.mixa@physik.uni-hamburg.de

- [1] P. Kapitza, *Viscosity of liquid helium below the λ -point*, Nature **141**, 74 (1938).
- [2] L. Landau, *Theory of the Superfluidity of Helium II*, Phys. Rev. **60**, 356 (1941).
- [3] G. E. Volovik, *The universe in a helium droplet*, (Oxford University Press, Oxford, 2003).
- [4] S. Stringari, and J. Treiner, *Systematics of liquid helium clusters*, J. Chem. Phys. **87**, 5021 (1987).
- [5] J. Dupont-Roc, M. Himbert, N. Pavloff, and J. Treiner, *Inhomogeneous liquid ^4He : A density functional approach with a finite-range interaction*, J. Low Temp. Phys. **81**, 31 (1990).
- [6] M. Casas, F. Dalfovo, A. Lastri, Ll. Serra, and S. Stringari, *Density functional calculations for ^4He droplets*, Z. Phys. D **35**, 67 (1995).
- [7] F. Dalfovo, A. Lastri, L. Pricauptenko, S. Stringari, and J. Treiner, *Structural and dynamical properties of superfluid helium: A density-functional approach*, Phys. Rev. B **52**, 1193 (1995).
- [8] D. S. Petrov, *Quantum Mechanical Stabilization of a Collapsing Bose-Bose Mixture*, Phys. Rev. Lett. **115**, 155302 (2015).
- [9] T. D. Lee, K. Huang, and C. N. Yang, *Eigenvalues and eigenfunctions of a Bose system of hard spheres and its low-temperature properties*, Phys. Rev. **106**, 1135 (1957).
- [10] C. R. Cabrera, L. Tanzi, J. Sanz, B. Naylor, P. Thomas, P. Cheiney, and L. Tarruell, *Quantum liquid droplets in a mixture of Bose-Einstein condensates*, Science **359**, 301 (2018).
- [11] G. Semeghini, G. Ferioli, L. Masi, C. Mazzinghi, L. Wolswijk, F. Minardi, M. Modugno, G. Modugno, M. Inguscio, and M. Fattori, *Self-bound quantum droplets of atomic mixtures in free space*, Phys. Rev. Lett. **120**, 235301 (2018).
- [12] T. G. Skov, M. G. Skou, N. B. Jørgensen, and J. J. Arlt, *Observation of a Lee-Huang-Yang fluid*, Phys. Rev. Lett. **126**, 230404 (2021).
- [13] I. Ferrier-Barbut, H. Kadau, M. Schmitt, M. Wenzel, and T. Pfau, *Observation of quantum droplets in a strongly dipolar Bose gas*, Phys. Rev. Lett. **116**, 215301 (2016).
- [14] M. Schmitt, M. Wenzel, F. Böttcher, I. Ferrier-Barbut, and T. Pfau, *Self-bound droplets of a dilute magnetic quantum liquid*, Nature **539**, 259 (2016).
- [15] L. Chomaz, I. Ferrier-Barbut, F. Ferlaino, B. Laburthe-Tolra, and B. L. Lev, and T. Pfau, *Dipolar physics: A review of experiments with magnetic quantum gases*, Rep. Prog. Phys. **86**, 026401 (2023).
- [16] R. Schützhold, M. Uhlmann, Y. Xu, and U. R. Fischer, *Mean-field expansion in bose-einstein condensates with finite-range interactions*, Int. J. Mod. Phys. B **20**, 3555 (2006).
- [17] A. R. P. Lima, and A. Pelster, *Quantum fluctuations in dipolar Bose gases*, Phys. Rev. A **84**, 041604(R) (2011).
- [18] A. R. P. Lima, and A. Pelster, *Beyond mean-field low-lying excitations of dipolar Bose gases*, Phys. Rev. A **86**, 063609 (2012).
- [19] F. Wächtler, and L. Santos, *Quantum filaments in dipolar Bose-Einstein condensates*, Phys. Rev. A **93**, 061603(R) (2016).
- [20] R. N. Bisset, R. M. Wilson, D. Baillie, and P. B. Blakie, *Ground-state phase diagram of a dipolar condensate with quantum fluctuations*, Phys. Rev. A **94**, 033619 (2016).
- [21] L. Santos, G. V. Shlyapnikov, and M. Lewenstein, *Roton-maxon spectrum and stability of trapped dipolar Bose-Einstein condensates*, Phys. Rev. Lett. **90**, 250403 (2003).
- [22] D. H. J. O’Dell, S. Giovanazzi, and G. Kurizki, *Rotons in Gaseous Bose-Einstein Condensates Irradiated by a Laser*, Phys. Rev. Lett. **90**, 110402 (2003).
- [23] L. Chomaz, R. M. W. van Bijnen, D. Petter, G. Faraoni, S. Baier, J. H. Becher, M. J. Mark, F. Wächtler, L. Santos, and F. Ferlaino, *Observation of roton mode population in a dipolar quantum gas*, Nat. Phys. **14**, 442 (2018).
- [24] D. Petter, G. Natale, R. M. W. van Bijnen, A. Patscheider, M. J. Mark, L. Chomaz, and F. Ferlaino, *Probing the roton excitation spectrum of a stable dipolar Bose gas*, Phys. Rev. Lett. **122**, 183401 (2019).
- [25] L. Tanzi, E. Lucioni, F. Famà, J. Catani, A. Fioretti, C. Gabbanini, R. N. Bisset, L. Santos, and G. Modugno, *Observation of a Dipolar Quantum Gas with Metastable Supersolid Properties*, Phys. Rev. Lett. **122**, 130405 (2019).
- [26] F. Böttcher, J.-N. Schmidt, M. Wenzel, J. Hertkorn, M. Guo, T. Langen, and T. Pfau, *Transient Supersolid Properties in an Array of Dipolar Quantum Droplets*, Phys. Rev. X **9**, 011051 (2019).
- [27] L. Chomaz, D. Petter, P. Ilzhöfer, G. Natale, A. Trautmann, C. Politi, G. Durastante, R. M. W. van Bijnen, A. Patscheider, M. Sohmen, M. J. Mark, and F. Ferlaino, *Long-Lived and Transient Supersolid Behaviors in Dipolar Quantum Gases*, Phys. Rev. X **9**, 021012 (2019).
- [28] D. S. Petrov and G. E. Astrakharchik, *Ultradilute Low-Dimensional Liquids*, Phys. Rev. Lett. **117**, 100401 (2016).
- [29] T. Ilg, J. Kumlin, L. Santos, D. S. Petrov, and H. P. Büchler, *Dimensional crossover for the beyond-mean-field correction in Bose gases*, Phys. Rev. A **98**, 051604(R) (2018).
- [30] F. Jia, Z. Huang, L. Qiu, R. Zhou, Y. Yan, and D. Wang, *Expansion dynamics of a shell-shaped Bose-Einstein condensate*, Phys. Rev. Lett. **129**, 243402 (2022).
- [31] R. H. Dicke, *Coherence in spontaneous radiation pro-*

- cesses, Phys. Rev. **93**, 99 (1954).
- [32] D. Nagy, G. Kónya, G. Szirmai, and P. Domokos, *Dicke-model phase transition in the quantum motion of a Bose-Einstein condensate in an optical cavity*, Phys. Rev. Lett. **104**, 130401 (2010).
- [33] K. Baumann, C. Guerlin, F. Brennecke, and T. Esslinger, *Dicke quantum phase transition with a superfluid gas in an optical cavity*, Nature **464**, 1301 (2010).
- [34] F. Mivehvar, F. Piazza, T. Donner, and H. Ritsch, *Cavity QED with quantum gases: new paradigms in many-body physics*, Adv. Phys. **70**, 1 (2021).
- [35] C. Emary, and T. Brandes, *Chaos and the quantum phase transition in the Dicke model*, Phys. Rev. E **67**, 066203 (2003).
- [36] R. Mottl, F. Brennecke, K. Baumann, R. Landig, T. Donner, and T. Esslinger, *Roton-type mode softening in a quantum gas with cavity-mediated long-range interactions*, Science **336**, 1570 (2012).
- [37] C. Maschler, I. B. Mekhov, and H. Ritsch, *Ultracold atoms in optical lattices generated by quantized light fields*, Eur. Phys. J. D **46**, 545 (2008).
- [38] S. B. Jäger, T. Schmit, G. Morigi, M. J. Holland, and R. Betzholz, *Lindblad Master Equations for Quantum Systems Coupled to Dissipative Bosonic Modes*, Phys. Rev. Lett. **129**, 063601 (2022).
- [39] L. Mixa, M. Radonjić, A. Pelster, M. Thorwart, *Engineering quantum droplet formation by cavity-induced long-range interactions*, arXiv:2409.18215 (2024).
- [40] D. Nagy, G. Szirmai, and P. Domokos, *Critical exponent of a quantum-noise-driven phase transition: The open-system Dicke model*, Phys. Rev. A **84**, 043637 (2011).
- [41] P. Zin, M. Pylak, and M. Gajda, *Revisiting a stability problem of two-component quantum droplets*, Phys. Rev. A **103**, 013312 (2021).
- [42] P. Karpov and F. Piazza, *Light-induced quantum droplet phases of lattice bosons in multimode cavities*, Phys. Rev. Lett. **128**, 103201 (2022).
- [43] N. Masalaeva, H. Ritsch, and F. Mivehvar, *Tuning Photon-Mediated Interactions in a Multimode Cavity: From Supersolid to Insulating Droplets Hosting Phononic Excitations*, Phys. Rev. Lett. **131**, 173401 (2023).